JMEPEG (2011) 20:1–10
DOI: 10.1007/s11665-010-9641-1

1059-9495/$19.00

Numerical and Experimental Investigation into Hot Forming of Ultra High Strength Steel Sheet

Hongsheng Liu, Wei Liu, Jun Bao, Zhongwen Xing, Baoyu Song, and Chengxi Lei

(Submitted August 25, 2009; in revised form February 6, 2010)

Hot forming of ultra high strength steel (UHSS) sheet metal grade 22MnB5 boron for channel components using water cooling is studied on a laboratory scale. After hot forming, the different microstructures such as martensite, bainite, and pearlite in formed component are produced, which are closely related with mechanical properties of formed component. The effect of forming start temperature and the contact state between blank and die on the microstructure evolution is investigated. In addition, the effect of processing parameters, such as forming start temperature and blank holder force (BHF), on the final quality of component, i.e., springback, that happens after hot forming of UHSS is investigated. It can be concluded that the forming start temperature has a significant effect on the final mechanical properties of formed components. The effect of forming start temperature on springback is examined in detail under a wide range of operating conditions. The higher the BHF and the forming start temperature, the lower is the springback after hot forming. Furthermore, thermo-mechanically coupled finite element analysis model encompassing heating of sheet blank, forming and quenching are developed for hot forming process. The stress distributions on sheet blank under different conditions during hot forming are compared to gain a fundamental understanding of the mechanism of springback. Comparisons show that numerical simulation results have good agreement with experimental results.

Keywords 22MnB5 steel, finite element analysis, hot forming, numerical simulation, springback

1. Introduction

Improvement in safety and the weight reduction of vehicles are required in order to comply with CO_2 emission regulations. One way to achieve emission targets is to use ultra high strength steels (UHSSs). However, it is clear that by increasing the strength of steel sheets, its formability deteriorates. In cold forming of the UHSS sheets, the springback is very large due to high strength-to-modulus ratio. Therefore, the use of UHSS sheets is still limited.

To improve the springback and formability of the UHSS sheets and to fabricate automobile structural components with tensile strength of 1500 MPa or more, hot forming is employed (Ref 1-4). Compared with conventional sheet metal forming, the proper hot forming process design, the knowledge of the interfacial phenomena, and material behavior at high temperatures are required to obtain the desired properties of the final products in terms of the microstructure, strength, and springback. During the hot forming process, the blanks are austenized and subsequently formed and quenched in the die (Ref 5). Forming and phase transformations are uniquely performed in a single step. Therefore, studying the mutual effects of deformation parameters and the possible phase transformations during the hot forming process on the final tensile strength of the formed components is of interest. It is evident that the mentioned phase transformations depend on several factors such as austenization schedules, chemical composition, and prior plastic deformations. The influence of austenization treatment (Ref 6) and plastic deformation of austenite before its transformation to matensite and bainite have been previously reported (Ref 7, 8). The large amount of springback after sheet forming of high-strength steels is one of the major problems. Generally, sheet metal forming at elevated temperatures (Ref 9) is effective in suppressing springback. With the aim of increasing formability, hot sheet metal forming has been investigated for steel (Ref 10); however, few investigations on hot sheet metal forming have been performed. In the present research, the influence of cooling rate and BHF on phase transformations and springback during hot sheet metal forming are investigated. The hot forming process is simulated using FE software ABAQUS. Numerical results are compared to experimental results to show the acceptable agreement.

Hongsheng Liu, Jun Bao, Zhongwen Xing, Baoyu Song, and **Chengxi Lei**, Department of Mechatronics Engineering, Harbin Institute of Technology, P.O. Box 425, Harbin 150001, P.R. China; and **Wei Liu**, Department of Materials Science and Engineering, Harbin Institute of Technology, P.O. Box 425, Harbin 150001, P.R. China. Contact e-mail: hs_liu_hit@163.com.

2. Experimental Procedure

The material used in this study is 22MnB5 steel, which represents the commonly used high strength in automotive industry. The chemical composition is listed in Table 1. The initial sheet thickness is 2.0 mm with base material being coated with an aluminum-silicon layer. In the as-delivered condition, the material exhibits a fine grain ferritic-pearlitic microstructure characterized by a good formability and a yield and tensile strength of about 400 and 600 MPa, respectively.

Martensitic transformation requires a minimum cooling rate of 27 K/s (Ref 11). To assure the appearance of the desired microstructural transformation, a previous austenitization of sheets above the material specific Ac3-temperature up to about 850 °C is essential. The furnace is a nonprotected atmosphere with maximum heating temperature of 1400 °C.

Tool system used in hot forming is shown in Fig. 1. The tool system mainly includes die, punch, and blank holder. All tools are cooled with integrated cooling holes. After forming, the component is cooled by means of cooled tools in order to achieve a structural change from austenite to martensite.

The stages of hot forming process as shown in Fig. 2 are: (1) heating of blank to 950 °C in a furnace; (2) transferring hot blank from the furnace to the die; (3) hot forming; and (4) quenching. The blank is austenized at 950 °C for about 180 s to guarantee a complete, homogenous austenitization. To keep high formability of sheet, the transfer time is controlled precisely to keep the forming start temperature high. The transfer time is suggested to be <6.5 s (Ref 12). In order to form the blank before the martensite start temperature is reached, the blank is formed within 0.9 s with punch velocity of 25 mm/s. Before and during the forming process, the temperature of sheet surface is recorded using a thermography camera. The schematic representation of the thermography camera positioning is illustrated in Fig. 3. The effect of cooling process on microstructure and tensile strength of formed component is considered. The rectangular specimens as shown in Fig. 4 taken from the bottom, the flange, and the sidewall of formed channel component, respectively, are used for investigation of microstructure and tensile strength.

Table 1 Chemical composition of the 22MnB5 steel (in mass%)

C	Si	Mn	P	S	Cr	Ti	B	N
0.23	0.22	1.18	0.015	0.001	0.16	0.04	0.003	0.005

3. FEM Modeling

Hot sheet metal forming is a thermo-mechanical forming process. In this case, a nonlinear, temperature-dependent, hardening function is required for describing plastic deformation of sheet metal in the simulation (Ref 13). The used material model is a temperature and strain-rate dependent elastic-plastic model. Influence of phase transformation and transformation plasticity is not considered in the model. In general, an explicit solution scheme is suitable for forming simulations to reduce computational cost and to relieve convergence problems. Hence, in this study a coupled thermal and mechanical analysis based on explicit time integration is used for both the modeling

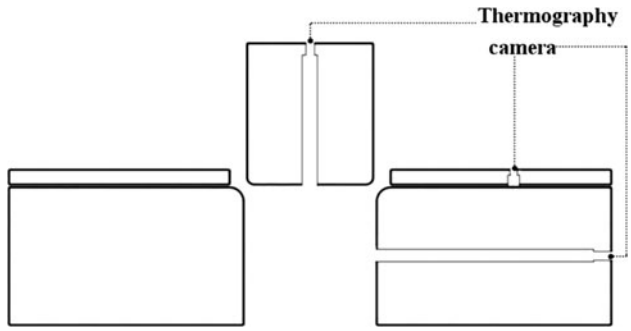

Fig. 3 Schematic of thermography camera positioning

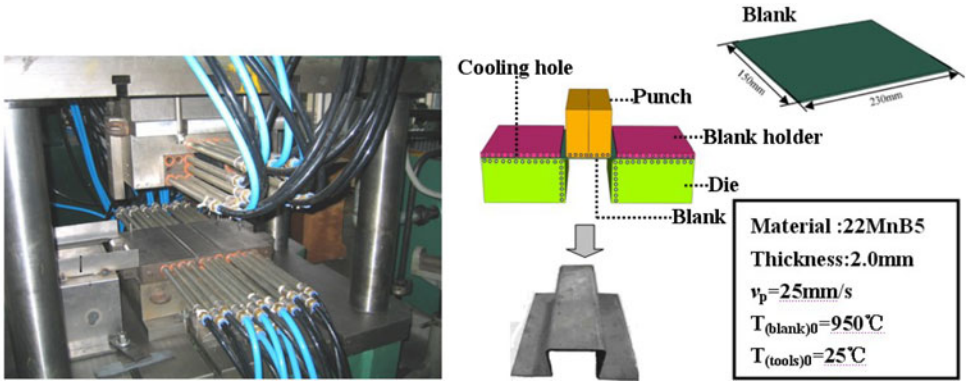

Fig. 1 Hot forming tool system

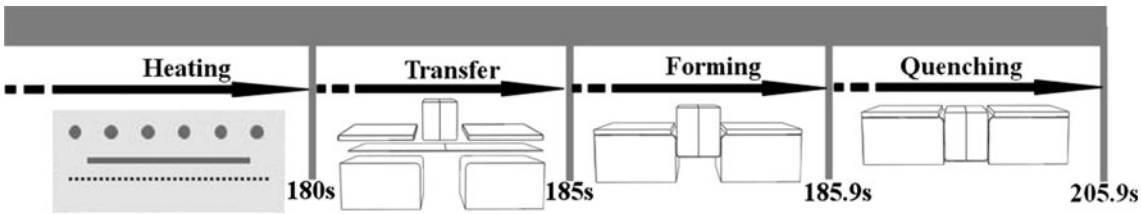

Fig. 2 Stages of hot forming process

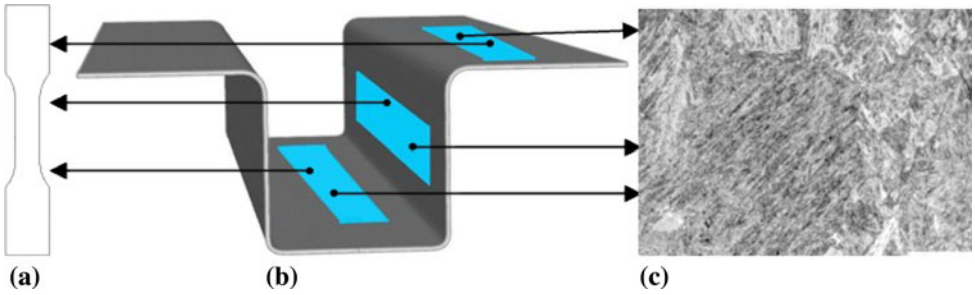

Fig. 4 Schematic of the tensile specimen and metallographic specimen. (a) Tensile specimen geometry, (b) three samples cut from the base of each formed component, and (c) metallographic specimen

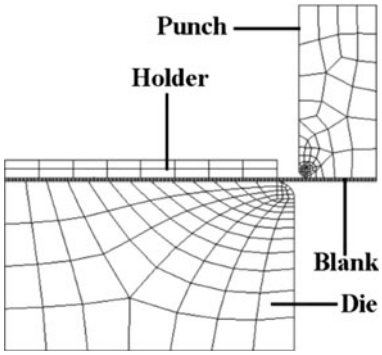

Fig. 5 FE mesh used for the simulation of hot metal sheet forming for channel component

of simultaneous forming and quenching using the commercially available FE package, ABAQUS/Standard. The modeled blank, die, and punch are corresponding to the experimental setup. Because of symmetry constraints, only half of blank and tools are modeled in the numerical simulation. To include the temperature effect in material deformation and interface condition, 2D plane strain solid element, CPE4RT owning both temperature and displacement degrees of freedom is used to describe the sheet blank. For simplicity, tooling elements are treated as rigid body. The finite element mesh of blank, punch, and die used in the simulation of the blank with 2.0 mm thickness is presented in Fig. 5. The mechanical contact between blank and tools is defined using a kinematic contact method. The friction force is modeled as rate-independent friction model with a static friction coefficient of $\mu = 0.1$. The punch has a velocity of 25 mm/s.

The hot sheet metal forming process is subdivided into three steps in the simulation. The first step is to transfer the blank from the furnace to the tool (<6.5 s). The second step is sheet forming. In the third step, quenching begins while the heat is transferred rapidly from blank to tools with cooling hole. During the transport, the blank loses heat by convection and radiation heat transfer to environment at 25 °C. The convection coefficients are calculated using the following standard empirical equations (Ref 14)

$$h_{\text{top}} = \left[0.14(\text{Gr} * \text{Pr})^{0.33}\right]\frac{k}{l} \quad \text{Blank top surface} \qquad \text{(Eq 1)}$$

$$h_{\text{bottom}} = \left[0.27(\text{Gr} * \text{Pr})^{0.25}\right]\frac{k}{l} \quad \text{Blank bottom surface} \qquad \text{(Eq 2)}$$

These equations are for turbulent free convection from a hot horizontal plate. The convection from the top surface is greater because the buoyancy driven flow is free to rise from the surface, where as it stagnates on the bottom surface. The properties of air for calculating the Grashof number, Gr, and the Prandtl number, Pr, are evaluated at the film temperature, T_{film}. L is a length scale. The convection heat transfer coefficient are $h_{\text{top}} = 18.3$ and $h_{\text{bottom}} = 41.26$ using Eq 1 and 2, respectively. A radiation conductance can be calculated using

$$h_{\text{rad}} = \frac{\sigma\varepsilon(T_1^4 - T_2^4)}{T_1 - T_2}, \qquad \text{(Eq 3)}$$

where $T_1 = T_{(\text{blank})0} = 950$ °C, $T_2 = T_{(\text{tools})0} = 25$ °C, $\sigma = 14.89 \times 10^{-8}$, and $\varepsilon = 0.8$. The radiation conductance $h_{\text{rad}} = 103.7$.

During hot sheet metal forming and quenching, the hot blank is placed on the die and cooled rapidly. The metal-to-metal thermal contact conductance is much greater than the convection and radiation coefficients. The thermal contact conductance $h(P)$ is calculated using the following equation (Ref 15)

$$h(P) = \frac{a}{b}\left[1 + 85\left(\frac{P}{c}\right)^{0.8}\right], \qquad \text{(Eq 4)}$$

where P is interface pressure. The parameters a, b, and c are defined in Ref 15.

The Young's modulus and Poisson's ratios as a function of temperature are taken from the literature (Ref 16). The plastic properties of 22MnB5 steel were obtained from the tensile tests in the literature (Ref 17) at temperatures varying from 500 to 900 °C and at strain rates of 0.1, 1.0, and 10.0 s^{-1} as illustrated in Fig. 6. Table 2 shows the detailed material properties and simulation conditions, and the isotropic behavior of this material is assumed.

4. Results and Discussion

4.1 Microstructure Evaluation

The critical issues during hot forming is the effect of forming start temperature and the contact between tools and blank on the microstructure of final component. The hot blanks are transferred from furnace to tools, and during this transfer the temperature of hot blank decrease. As a result, hot forming is not performed at the austenization temperature, but instead at

lower temperature. The effect of forming start temperatures on phase transformation is investigated in this study. Forming start temperatures from 700 to 950 °C are selected below austenization temperature. Other forming variables are not changed. Three light optical microscopy images, representing different microstructures in the flange of formed component at different forming start temperatures of 950, 850, and 700 °C, are given in Fig. 7. The microstructure as shown in Fig. 7(a) is fully martensitic while the fraction of martensite decreases with the forming start temperature increasing. The microstructure in the flange of formed component is mixture of martensite and bainite, and the variation in the fraction of martensite and bainite is shown in Fig. 8. From Fig. 8, it can be observed that in the flange the fraction of martensite increases about 35% by increasing the forming start temperature from 700 to 950 °C. On the contrary, the fraction of bainite decreases about 35%. Tensile tests are performed to evaluate the tensile strength of the flange, and the tensile strengths-forming start temperature

Table 2 Material properties and simulation conditions

Material	22MnB5
Dimensions	
Thickness	2.0 mm
Length	230 mm
Width	150 mm
Properties	
Density (kg/m^3)	7830
Linear expansion (1/°C)	1.3e−05
Young's modulus (GPa)	100.0
Poisson's ratio	0.3
Simulation conditions	
Punch speed (mm/s)	25
Tool temperature (°C)	25
Thermal contact conductance (W/m^2 K)	2000
Convection heat transfer coefficient (W/m^2 K)	8.3
Radiation conductance (W/m^2 K)	107
Friction coefficient	0.1

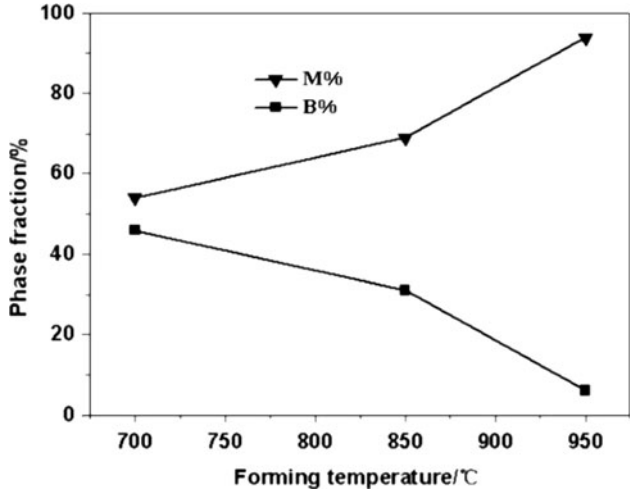

Fig. 8 The effect of forming start temperature on the microstructure of formed part in the flange

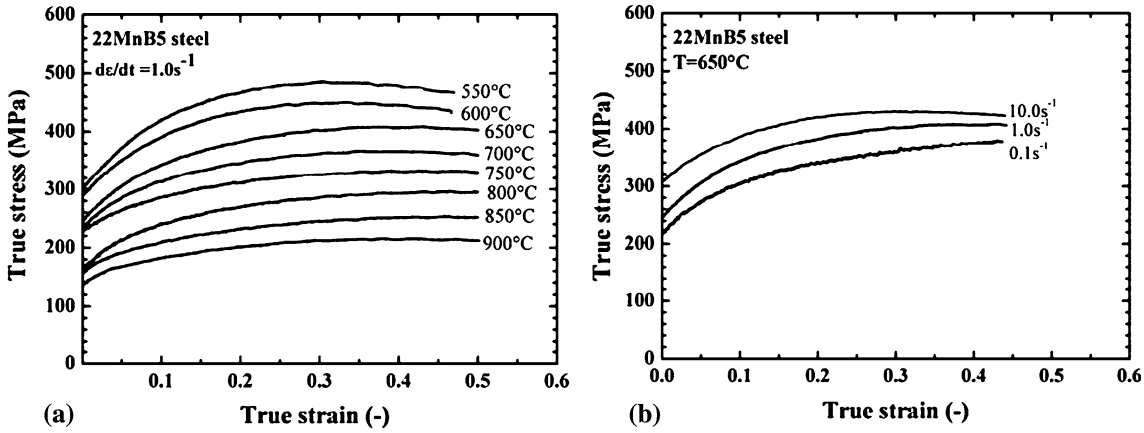

Fig. 6 True stress-strain curve of 22MnB5 in various temperatures and strain rates (Ref 18)

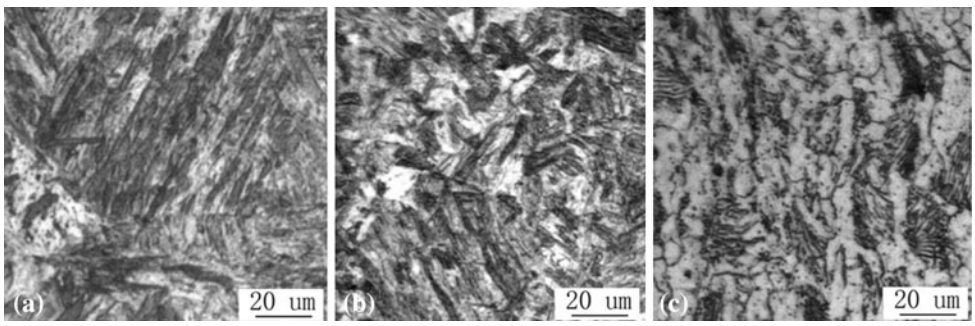

Fig. 7 Optical micrographs of final specimens formed at forming start temperatures: (a) 950 °C, (b) 850 °C, and (c) 700 °C in the flange

curves are shown in Fig. 9. The curve characteristics show that the forming start temperature has a significant influence on the tensile strength of formed component. Decreasing the forming start temperature leads to a significant reduction of tensile strength.

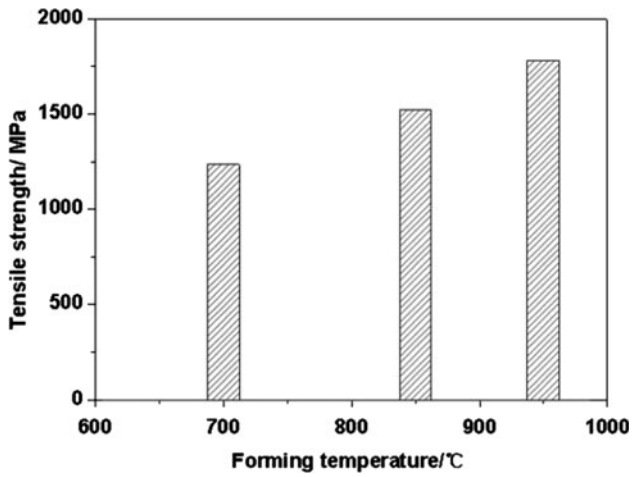

Fig. 9 The effect of forming start temperature on tensile strength of formed part in the flange

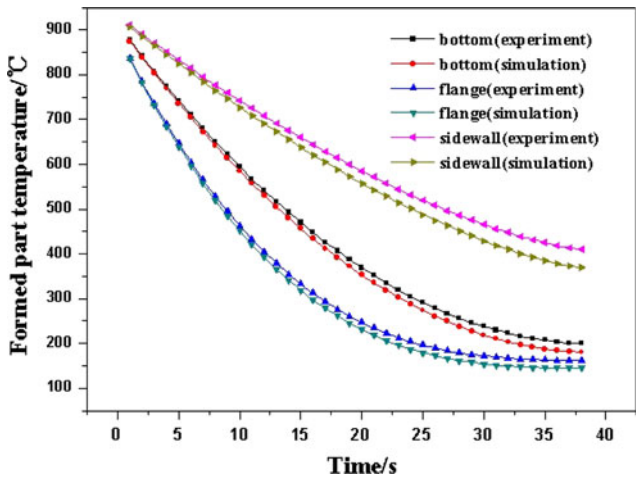

Fig. 10 The variation in temperatures in zones of the flange, the bottom and side wall (forming start temperature of 950 °C)

The heat transfer is a key process affecting the evolution of the mechanical properties of formed component, and the thermal contact is an important factor influencing the final microstructure of formed component. During the quenching, the contact state between formed channel component and tools is variable. Due to the gap between the die and the punch, the sharp decrease of real contact area on the sidewall of formed component leads in general to a reduced heat transfer. The sidewall loses heat by convection and radiation heat transfer to the environment at 25 °C. The well contact between the flange and the die improves the heat transfer from the flange to the die, as a result, the flange loses heat by thermal contact, and the bottom loses heat in the same way. As results of the fact that metal-to-metal thermal contact conductance is much greater than the convection and radiation coefficients, during the quenching the temperatures in the flange and the bottom decrease sharply, on the contrary, the side wall is cooled at lower cooling rate. During the quenching, the variation in temperatures of the flange, the sidewall, and the bottom is shown in Fig. 10. Figure 10 shows that the flange is cooled at the highest rate in the three zones. At the end of quenching, the temperature of the flange is the lowest. As a consequence, the flange is hot treated fully and the mechanical property of the flange is improved (see Fig. 9). Figure 10 also shows a good agreement between the numerical simulation results and the experimental results as well as the reliability of FE model built up in this work in simulation of hot sheet metal forming.

For the forming start temperature of 950 °C, the microstructures of final formed component are given in Fig. 11. It is observed that the bad contact state during the process of hot forming for channel component results in coarse martensite grain in the bottom and fine martensite grain in the flange as well as coarse upper bainite grain in the sidewall.

4.2 Springback

4.2.1 Definition of Springback. The dimensional accuracy after springback is evaluated by three geometric quantities as illustrated in Fig. 12: the angle between the bottom and the sidewall (θ_1), the angle between the flange and the sidewall (θ_2), and the residual curvature ($\kappa = 1/\rho$) of the sidewall. In the ideal cases of no springback, 90° of θ_1 and θ_2 and the flat sidewall ($\kappa = 0$) are expected.

The detailed information about the component shape can be obtained in FEA from the coordinate of each blank element, the angles of blank elements with the bottom of the sheet (angle α) and with the flange of the sheet (angle β) are obtained, respectively, after reaching the equilibrium state as shown in Fig. 13. Since the drastic change of slope in α and β is observed

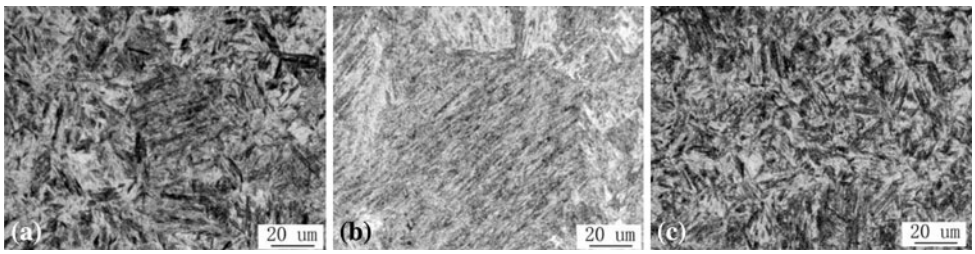

Fig. 11 Optical micrographs of final specimens formed at forming temperature of 950 °C at three zones: (a) the bottom, (b) the sidewall, and (c) the flange

at the points L and U around the punch and die corner regions, these two points could be regarded as the boundaries between the sidewall and the punch and die corner regions, respectively. Hence, as three geometric parameters characterizing the springback amount of a component, the angle θ_1 is obtained from the angle α at the point L, and the angle θ_2 from the angle β at the point U. The sidewall curvature (κ) is calculated using the difference of the angle α or β and the distance between the points L and U. By eliminating the mixed effect of two quantities in obtaining the springback amount using the proposed measuring method, it is expected that the effects of process parameters on the springback behavior can be analyzed more accurately under a wide range of operating conditions.

4.2.2 Effect of Forming Start Temperature on Springback. The effect of forming start temperature on the amount of springback is studied under the nonisothermal temperature conditions where the blanks are formed at different forming start temperatures of 700, 800, 900, and 950 °C. From the final component shape shown in Fig. 14(a) after springback with different forming start temperatures, the reduction tendency of springback at elevated forming start temperatures could be observed. The amount of springback is illustrated in Fig. 14(b).

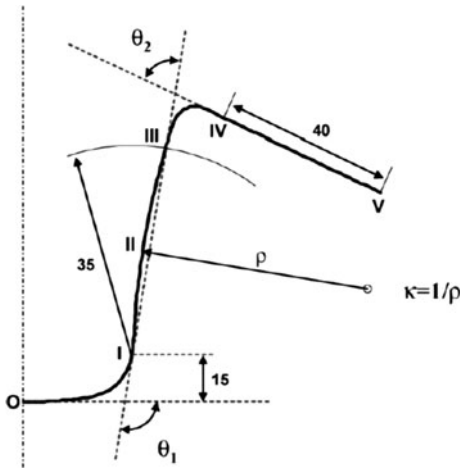

Fig. 12 Three quantities characterizing springback (Ref 18)

In the case of angle θ_1 between the bottom and the sidewall, the decreased springback angle ($\Delta\theta_1$) from 3.65 to 1.23 is observed as forming start temperature increased from 700 to 950 °C. However, the angle θ_2 between the flange and the sidewall is not very sensitive to forming start temperature. Very small springback amount ($\Delta\theta_2$ of −0.26° to 0.03°) is obtained in the temperature range of 700-950 °C. On the other hand, the curvature of the sidewall is strongly affected by forming start temperature. The curvature change ($\Delta\kappa$) after springback could be remarkably reduced almost to the zero level by increasing the forming start temperature up to 950 °C.

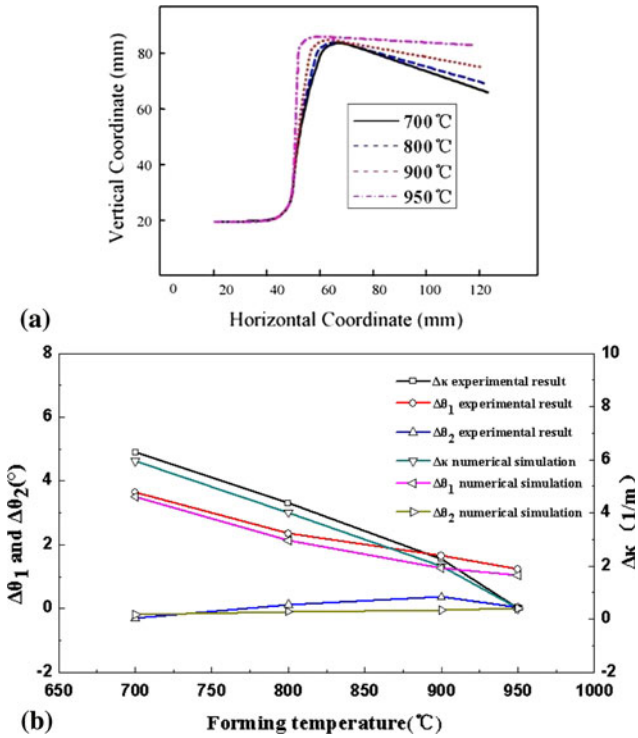

Fig. 14 Effect of forming start temperature on the springback in nonisothermal conditions: (a) variation of part shape and (b) variation of the springback amount in each point region

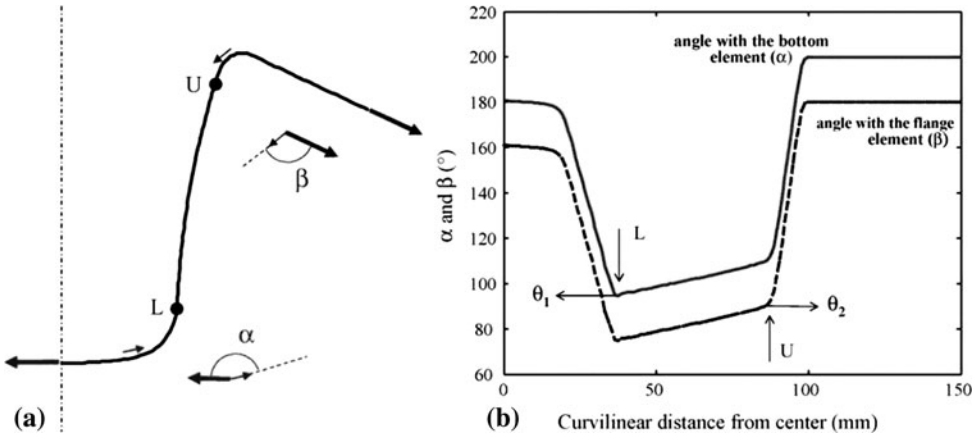

Fig. 13 Measuring method for springback characterization in FEA: (a) a sketch to define α and β and (b) variation of α and β after springback

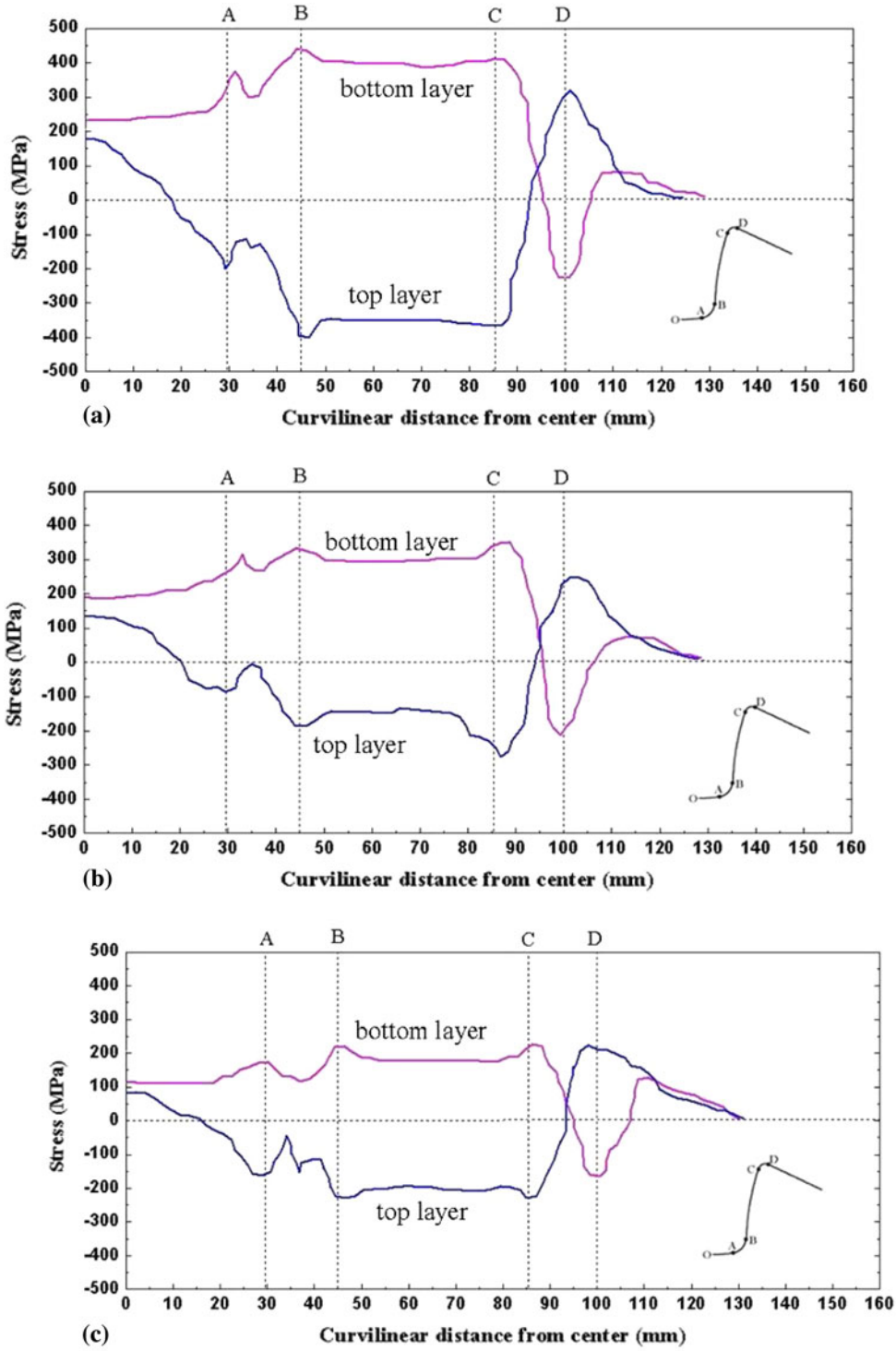

Fig. 15 Stress distribution of the blank in nonisothermal conditions (BHF = 1.6 kN): (a) T = 700 °C, (b) T = 800 °C, and (c) T = 950 °C

To further investigate the reason for the springback reduction at elevated forming start temperatures, stress distribution of the component before unloading is examined by defining local coordinate system in the FEA model and measuring the normal component of stresses of each blank element. The variation of stresses on the top and bottom layers of blank elements is shown in Fig. 15 in each distinct tooling region (i.e., AB: punch corner, BC: sidewall, and CD: die corner). Since the punch corner region (AB in Fig. 15) mainly experienced bending tension, the bottom layer of this region is exerted with tensile stress, while the top layer is exerted compressive stresses. The decrease of stress magnitude in the middle layer seems to be due to the unbending effect. In addition, it is found that the difference of tensile and compressive stresses became smaller as forming start temperature increasing due to the decreased tensile strength of 22MnB5 at elevated forming start

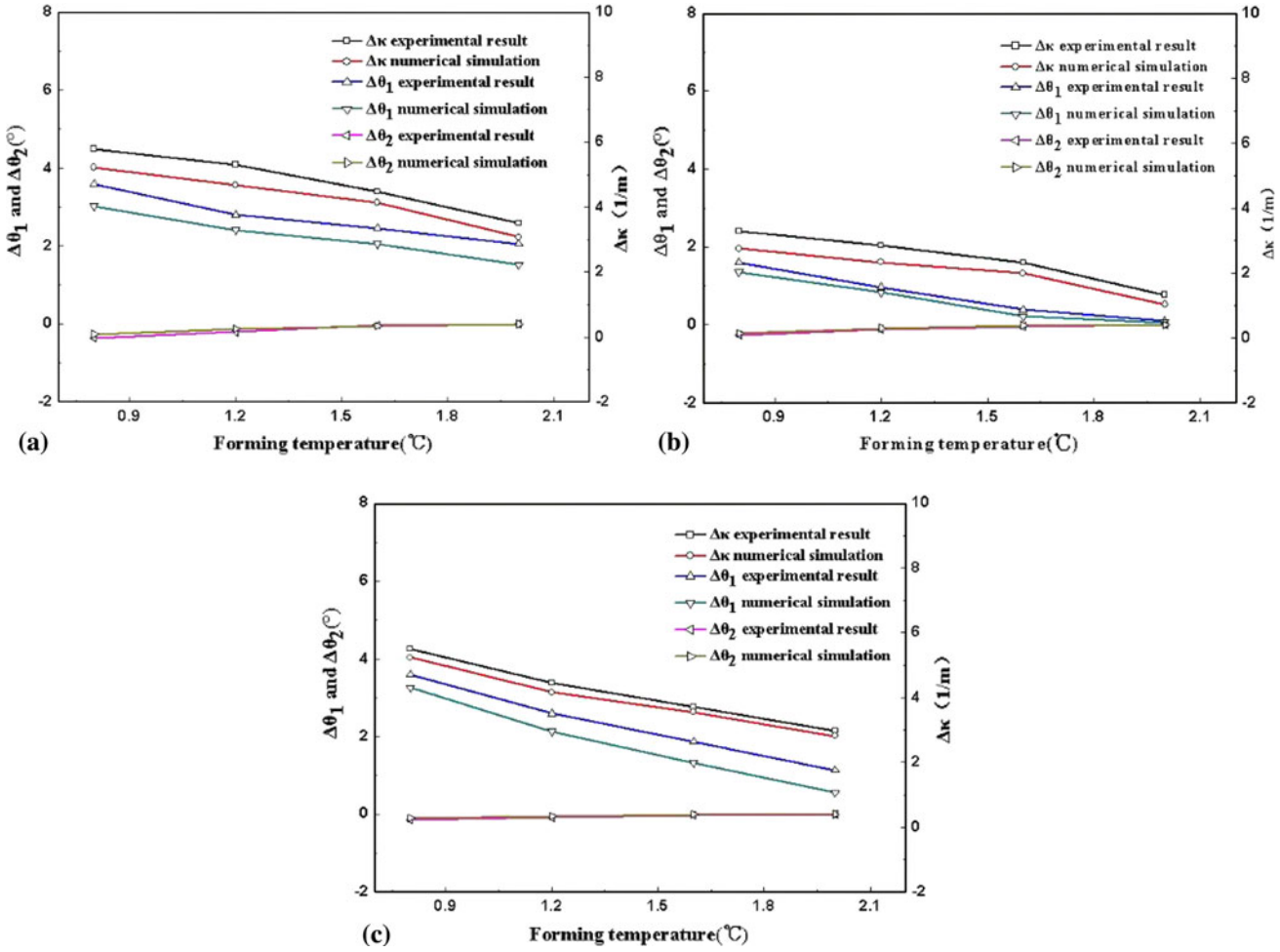

Fig. 16 Effect of BHF on springback: (a) T_{die} = 25 °C and T_{punch} = 25 °C, (b) T_{die} = 250 °C and T_{punch} = 250 °C, and (c) T_{die} = 250 °C and T_{punch} = 25 °C

temperatures, which resulted in smaller residual bending moment after hot forming. As a result, at forming start temperature of 950 °C, the top and bottom layers are mainly in the tensile region, and much more reduced springback amount ($\Delta\theta_1$ = 1.23°) is obtained.

For the elements in the sidewall region (BC in Fig. 15) that experienced more complicated bending, unbending, and reverse bending under tension, large amount of tensile and compressive stresses are observed in the bottom and top layers of the blank, respectively, at forming start temperature of 700 °C (Fig. 15a). The stress characteristic before unloading led to large bending moment, hence large amount of springback in this region. However, at forming start temperature of 800 °C (Fig. 15b), it is observed that the overall stress level decreased with forming start temperature increasing because the material strength decreased at elevated forming start temperatures. Therefore, the curvature change of the sidewall could be significantly reduced at elevated forming start temperatures. It is also found that the magnitude of both tensile and compressive stresses decreased in the middle layer, especially in high forming start temperature conditions. It seems to be due to the reverse bending effect to keep the sidewall straight during forming. As forming start temperature increased, its effect became more pronounced due to the decreased strength level and the increased ductility of the material. At forming start temperature of 950 °C (Fig. 15c), the stresses of blank elements are mostly in tensile condition, and in some locations, the top layer is exerted with larger tensile stresses than the bottom layer. As a result, further reduced curvature change of <0.65 m^{-1} after springback could be achieved as shown in Fig. 14(b).

In the case of die corner region (CD in Fig. 15), it is noted that the stress state changed from tension to compression for the bottom layer and compression to tension for the top layer. Even though the region is affected by the bending on the die profile radius, its effect is almost vanished at the entrance of the sidewall region (i.e., point C). Instead, the opposite stress condition caused by unbending is developed due to the interaction with the sidewall elements. Since the bending moments caused after hot forming at the points C and D are in the same direction, the springback amount ($\Delta\theta_2$) determined by the difference of these two bending moments are not very significant in all temperature conditions as illustrated in Fig. 14(b). Consequently, θ_2 is not a sensitive factor to forming start temperatures and the springback amount of this region is found to be negligible.

In summary, the springback amount of the angle θ_1 and the sidewall curvature (κ) could be greatly reduced by increasing forming start temperature. However, the angle θ_2 between the

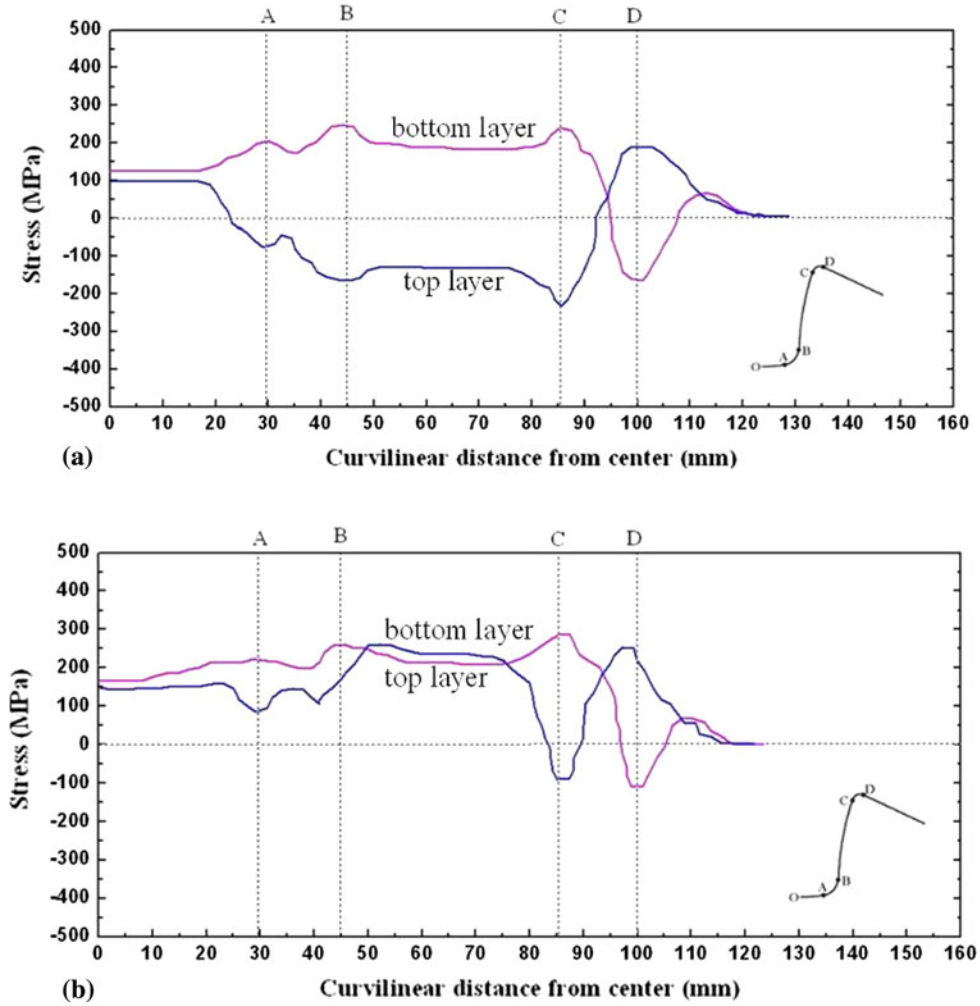

Fig. 17 Stress distribution of the blank at various BHFs (T = 950 °C): (a) BHF = 1.2 kN and (b) BHF = 2.0 kN

flange and the sidewall showed the negligible springback regardless of temperature condition for the given material and tooling geometry. Therefore, it can be confirmed that hot forming is a promising technology to secure the dimensional accuracy of a formed component as well as to improve the formability of advanced high-strength materials.

4.2.3 Effect of BHF on Springback. As one of the sensitive factors affecting the component quality in hot forming, the effect of blank holder force (BHF) on springback is investigated at three different temperature conditions (i.e., room temperature, isothermal heating condition (T_{die} and T_{punch} = 250 °C), and nonisothermal heating condition (T_{die} = 250 °C and T_{punch} = 25 °C). As shown in Fig. 16, in all temperature conditions, it is found that the angle θ_1 and the sidewall curvature (κ) are strongly affected by the BHF. The springback reduction with increasing BHF is observed. However, for the similar reason explained in the previous section, the angle θ_2 shows the negligible amount of springback in all cases. The trend of springback reduction with increasing BHF could be explained from a simple moment-curvature relationship. The bending moment required to achieve a given curvature decreases with increasing tension (Ref 18). Hence, for higher BHF, the corresponding added tension is higher, thus the springback amount after elastic unloading is reduced. The stress distribution on the top and bottom layers of the sheet for two different BHF values when forming start temperature equals to 250 °C is illustrated in Fig. 17. It could be seen that with BHF increasing, the compressive stress on the top layer of the sheet shift up to the tensile stress due to the reduced magnitude of bending moment and the increased tensile stress. Thus, the stresses in the thickness direction are almost uniform except for the die corner region (CD). The improved dimensional accuracy after springback could be achieved for higher BHF due to these facts that the uniform stress distribution helps to reduce the springback and the increased tensile stress leads to more larger ratio of plastic deformation of total deformation and more smaller elastic deformation, which results in more smaller springback.

5. Conclusions

The effect of the process parameters on the martensitic transformation during hot forming is studied. A large number of experiments for different deformation conditions have been performed to reveal the effects of relevant process parameters on the martensitic transformation, the tensile strength of hot

formed component, and the final component quality in the 22MnB5 steel grade.

Considering the results achieved using the experimental and numerical simulation methods, it is concluded that:

1. The higher forming start temperature resulted in a higher volume fraction of martensite in formed component and therefore higher tensile strength. By increasing the forming start temperature from 700 to 950 °C, the fraction of martensite increased by 35%, the tensile strength of formed increased by 550 MPa. In addition, the effect of contact between blank and tools on the cooing rate of blank during the hot forming and thus the microstructure of formed component is obvious, the microstructure in the flange is fully transformed into martensite, and the microstructure in the sidewall is mixture of martensite and bainite.
2. The springback amount is greatly reduced by increasing the forming start temperature from 700 to 950 °C due to the decreased material strength at elevated temperature. The springback reduction is pronounced in the sidewall and punch corner regions. However, the springback in the die corner is negligible due to the increased unbending effect near the sidewall region. It can be concluded that the elevated temperature in the hot sheet metal forming leads to the improvement of the dimensional accuracy as well as the formability of sheets of grade 22MnB5 boron steel.
3. The increased level of BHF can help to reduce the springback amount. Since the required bending moment for a given curvature is relatively lower when higher tensile stress is applied to the blank, the stresses along the thickness direction developed after hot sheet metal forming showed more uniform characteristic and corresponding bending moment can be significantly reduced. However, since higher restraining force has a negative effect on the formability of 22MnB5 materials, an appropriate compromise is required to determine the optical levels of these factors.

Acknowledgments

This work is made possible by supports from natural science foundation of Heilongjiang Province China under Grant No. QC07C07 and China Postdoctoral Science Foundation under Grant No. 20080440846.

References

1. L. Vaissiere, J.P. Laurent, and A. Reihardt, Development of Pre-Coated Boron Steel for Applications on PSA Peugeot Citroen and RENAULT Bodies in White, *J. Mater. Process. Technol.*, 2003, **111**, p 909–917
2. R. Kolleck, D. Steinhoefer, J.A. Feindt, and P. Bruneau, Manufacturing Methods for Safety and Structural Body Components for Lightweight Body Design, *IDDRG, Conf. Proc.*, 2004, p 167–173
3. L. Garcia Aranda, P. Ravier, and Y. Chstel, Hot Stamping of Quenchable Steels, Material Data and Process Simulations, *IDDRG, Conf. Proc*., 2003, p 155–164
4. L. Gehringhoff, High Strength Hot Stamped Parts for Body Structures, New Advances in Body Engineering, *Euromotor Course*, IKA RWTH Aachen, 2004, p 1–15
5. M. Merklein, C. Hoff, and J. Lechler, Einflussgrößen im Presshartprozess, *Tagungsband 4*, Chemnitzer Karosseriekolloquium, Chemnitz, Germany, 2005, p 137–153
6. M. Geiger, M. Merklein, and C. Hoff, Basic Investigations on the Hot Stamping Steel 22MnB5, *Adv. Mater. Res.*, 2005, (6–8), p 795–804
7. S. Chatterjee, H.S. Wang, J.R. Yang, and H.K.D.H. Bhadeshia, Mechanical Stabilisation of Austenite, *Mater. Sci. Technol.*, 2006, **22**(6), p 641–644
8. M. Naderi and W. Bleck, Martensitic Transformation during. Simultaneous High Temperature Forming and Cooling Experiments, *Steel Res. Int.*, 2007, **78**(12), p 914–920
9. R. Neugebauer, T. Altan, T. Geiger, M. Kleiner, and A. Sterzing, Sheet Metal Forming at Elevated Temperature, *Ann. CIRP.*, 2006, **55**(2), p 793–816
10. F. Vollertsen and K. Lange, Enhancement of Drawability by Local Heat Treatment, *Ann. CIRP.*, 1998, **47**(1), p 181–184
11. M. Merklein and J. Lechler, Investigation of the Thermo-mechanical Properties of Hot Stamping Steels, *J. Mater. Process. Technol.*, 2006, **177**, p 452–455
12. B. Shapiro, Using Ls-Dyna to Model Hot Sheet Metal Forming, *First International Conference on Hot Sheet Metal Forming of High-Performance Steel*, Kassel, Germany, 2008
13. M. Eriksson, M. Oldenburg, M.C. Somani, and L.P. Karjalainen, Testing and Evaluation of Material Data for Analysis of Forming and Hardening of Boron Steel Components, *Modell. Simul. Mater. Sci. Eng.*, 2002, **10**, p 1–18
14. W.H. McAdams, *Heat Transmission*, 3rd ed., McGraw Hill, New York, 1954, p 180
15. L. Sellers, *Proc. of 2nd Int. Conf. Modeling of Metals Rolling Processes*, The Institute of Materials, London, 1996
16. R.D. Pehlke, A. Jeyarajan, and H. Wada, *Summary of Thermal Properties for Casting Alloys and Mold Materials*, University of Michigan, Ann Arbor, MI, 1982
17. M. Naderia, L. Durrenberger, A. Molinarib, and W. Blecka, Constitutive Relationships for 22MnB5 Boron Steel Deformed Isothermally at HighTemperatures, *Mater. Sci. Eng. A*, 2008, **478**, p 130–139
18. M.G. Lee, D. Kim, C. Kim, M.L. Wenner, and K. Chung, Spring-back Evaluation of Automotive Sheets Based on Isotropic-kinematic Hardening Laws and Non-quadratic Anisotropic Yield Functions. Part III. Applications, *Int. J. Plast.*, 2005, **21**, p 915–953